

Solute Trapping and the Effects of Anti-Trapping Currents on Phase-Field Models of Coupled Thermo-Solutal Solidification

A.M. Mullis^{§}, J. Rosam^{§‡} & P.K. Jimack[‡]*

Institute for Materials Research[§] and School of Computing[‡],

University of Leeds, Leeds LS2 9JT, UK.

Abstract

We explore how the inclusion of an anti-trapping current within a phase-field model of coupled thermo-solutal growth formulated in the thin interface limit actually affects the observed levels of solute trapping during dendritic growth. The problem is made computational tractable by the use of advanced numerical techniques including local mesh adaptivity, implicit temporal discretization and a multigrid solver. Contrary to published results for pure solutal models we find that the inclusion of such an anti-trapping current does not lead to the recovery of the equilibrium partition coefficient, except in the limit of very slow growth. At higher growth velocities non-vanishing amounts of solute trapping are observed.

Key Words: A1. Computer Simulation, A1. Dendrites, A2. Growth from Melt, B1. Alloys.

PACS: 81.30.Fb

* Corresponding Author, e-mail : A.M.Mullis@leeds.ac.uk

tel : +44-113-343-2568

fax : +44-113-343-2384

1. Introduction

Dendritic growth has been a subject of enduring scientific interest, both because it is a prime example of spontaneous pattern formation and due to the propensity of many metals to solidify dendritically from their parent melt. Moreover, remnants of these dendritic microstructures often survive subsequent processing operations, such as rolling and forging and thereafter have a pervasive influence on the engineering properties of these metals.

In recent years significant progress towards understanding dendritic growth has been afforded by phase-field modelling. However, the application of phase-field modelling has largely been restricted to two limiting cases; namely the thermally controlled growth of pure substances [e.g. 1, 2] and the solidification of relatively concentrated alloys and solutions [e.g. 3, 4], wherein growth is sufficiently slow that the problem may be considered isothermal. However, in the cases of the solidification of very dilute alloys and of rapid solidification processing the isothermal approximation is no longer valid and it becomes necessary to solve the problem for coupled heat and solute transport.

Two basic formulations of the coupled phase-field problem have been reported in the literature. The first, which is due to Loginova *et al.*^[5], follows on from the derivation of the solutal model of Warren & Boettinger^[6]. However, there are doubts about the quantitative validity of this model^[7] as the numerical results display excess solute trapping and have an unresolved interface width dependence. This methodology has been extended numerically by Lan *et al.*^[8], who introduced an adaptive finite volume solver, which allowed them to use realistic values of the Lewis number (Le = ratio of thermal to solutal diffusivity), Le , although this did not overcome either the excess solute trapping or the interface-width dependence observed in the solution. An alternative formulation of the coupled phase-field problem based on the Karma thin interface model^[9] has been presented by Ramirez & Beckermann^[7, 10] and has been extended numerically by ourselves^[11, 12] to incorporate a fully adaptive, fully implicit, multigrid solver, allowing higher Lewis numbers and lower undercoolings to be studied. As the thin interface model has been shown to be independent of the length scale chosen for the mesoscopic diffuse interface width, it is capable of giving quantitatively correct predictions for dendritic growth velocity, V , and tip radius, ρ . Moreover, the inclusion of an anti-trapping current^[9] within this

formulation of the coupled problem should ensure that the problems associated with *excess* solute trapping observed in the models of [5, 8] are overcome.

During equilibrium solidification solute will partition between the solid and the liquid such that the concentrations, c_s^0 and c_l^0 , at the interface location in the solid and liquid phases respectively are in a fixed ratio,

$$k_E = \frac{c_s^0}{c_l^0} \quad (1)$$

where k_E is the equilibrium partition coefficient and can be obtained from the location of the liquidus and solidus lines on the phase diagram. This partitioning of solute ensures that the chemical potentials on either side of the interface remain equal (local equilibrium). However, as we depart from equilibrium by increasing the growth velocity, V , either by undercooling the melt or by imposing large thermal gradients to effect rapid heat extraction, the actual ratio c_s^0 / c_l^0 moves away from k_E and begins to approach 1. This process of solute trapping has been shown by Aziz^[13, 14] to give rise to a velocity-dependant partition coefficient, $k(V)$, which may be described as

$$k(V) = \frac{k_E + \beta}{1 + \beta} \quad (2)$$

where β is a dimensionless growth velocity which is generally written as either $\beta = V/V_D$, where V_D is a characteristic diffusive velocity for atoms at the solid-liquid interface, or as $\beta = VW_p/D_i$, where W_p is a measure of the physical width of the solid-liquid interface and D_i is an interface diffusion coefficient. In this latter case β takes the form of an interface Péclet number.

In this paper we will use a phase-field model of coupled thermo-solutal growth for dendrites of a dilute binary alloy into their undercooled parent melt in order to study the solute trapping phenomenon. Our objectives are twofold; firstly, to use our phase-field model as a mechanism to study the solute trapping phenomenon and secondly to understand specifically how the inclusion of anti-trapping currents effects the behaviour of the coupled thermo-solutal model. The first of these two themes has been addressed by a number of authors previously whilst the second, as far as we are aware, has not been discussed elsewhere. For the

growth of a dendrite under *solute only control* it was shown in [9] that the inclusion of an anti-trapping current effectively totally suppresses solute trapping. However, the growth velocities observed for solutal dendrites may be very low compared to that for dendrites growing under coupled thermo-solutal control, and consequently it is not clear what effect the inclusion of an anti-trapping current within a coupled thermo-solutal model of dendritic growth will have.

Where phase-field models of solidification have previously been used to study solute-trapping, it is generally by means of a 1-dimensional model which is either isothermal (e.g. [15, 16, 17, 18, 19]) or such that a constant temperature gradient is imposed (e.g. [20]). In [18] and [19] a thin-interface analysis (matched asymptotic analysis in the inner and outer regions) has been applied and where this is the case quantitatively valid extension of the model to more than 1-dimension should be possible (i.e. prediction of dendrite growth velocity and radius of curvature are possible as the results are independent of the width assumed for the diffuse interface). For the other models cited above, which do not use the thin interface formulation, this is not the case as the results of such simulation would be expected to show an unresolved dependence on the interface width. In all cases the diffusion of heat is ignored. However, the validity of working in the isothermal limit is far from clear to us. Specifically, one would expect to see significant solute trapping only during rapid solidification. These are precisely the conditions under which the thermal field generally cannot be ignored. The underlying assumption behind the isothermal model is that growth is so slow that no temperature gradients are present in the melt ahead of the growing solid. This ceases to be true once appreciable levels of solute trapping are present. In particular, as $k \rightarrow 1$ the interface temperature, T_i , drops rapidly with velocity (see for instance Figures 3 & 6 in [16] where T_i has been estimated from an asymptotic analysis or Figure 4 in [20] where T_i has been measured directly from the imposed thermal gradient). This drop in T_i is equivalent to an increase in the thermal undercooling, ΔT , and represents the transition in the rate limiting process from solutal to thermal diffusion. Yet in the isothermal model this process is absent.

In this paper we present the results of a phase-field investigation in which we use the coupled thermo-solutal model due to Ramirez *et al.*^[10] to study solute trapping during rapid solidification. In this model the diffusion of latent heat is properly accounted for. The model is formulated in the thin interface limit to remove interface width dependencies from the solution and uses the standard thin-interface assumptions of no interface

kinetics, symmetric thermal diffusivities (i.e. thermal diffusivity equal in the solid and liquid phases) and asymmetric solute diffusivity (i.e. zero solute diffusivity in the solid).

2. Description of the Model

The coupled thermo-solutal phase-field model for solidification used in this work is that first proposed by Ramirez *et al.* ^[10]. Although we do not seek here to present again the derivation of this model in full, some details of the derivation are necessary to understand the implications of the finding presented later. The starting point for the model is the definition of a free energy functional,

$$F = \int_V f(\phi, c, T) + \frac{\sigma}{2} |\nabla \phi|^2 dV \quad (3)$$

where $\phi(\mathbf{x}, t)$ is the phase variable, which takes values +1 in the solid phase and -1 in the liquid phase, $c(\mathbf{x}, t)$ is the local concentration of component B in A , T is the absolute temperature and σ_ϕ is related to the width of the diffuse interface, W , via the relation $\sigma = W^2 H$, where H is the height of the double-well potential barrier between the solid and liquid phases. $f(\phi, c, T)$ is the local free energy, the form of which is discussed in detail in [10] and [21]. Here, we distinguish between W , the width of the diffuse interface in the phase-field simulation and W_p , its physical counterpart determined by the number of atom planes over which the transition from full long-range ordering in the solid to the absence of long-range order in the liquid is accomplished. This is because, although ideally $W \rightarrow W_p$, for computational expediency there may be instances where this is not the case.

The evolution of the phase and concentration fields are given by

$$\frac{\partial \phi}{\partial t} = -K_\phi(T) \frac{\delta F}{\delta \phi} \quad (4)$$

and

$$\frac{\partial c}{\partial t} = \nabla \cdot \left(K_c \nabla \frac{\delta F}{\delta c} - j_{at} \right) \quad (5)$$

where K_ϕ is the atomic mobility at the interface and

$$K_c = \frac{V_0}{RT_M} Dq(\phi)c \quad (6)$$

where D is the diffusivity of the solute in the liquid phase and $q(\phi)$ is an interpolating polynomial that describes how the diffusivity varies across the solid-liquid interface. For an asymmetric system, which is appropriate to solute transport (i.e. the diffusivity in the solid is very much smaller than that in the liquid), we require $q(1) = 0$ and $q(-1) = 1$.

Here the first term inside the bracket in Eq. (5) is a manifestation of Fick's law for diffusion in the liquid while the second term is an anti-trapping current as first proposed by [9],

$$j_{at} = -ac_\infty(1-k_E)We^u \frac{\partial \phi}{\partial t} \frac{\nabla \phi}{|\nabla \phi|} \quad (7)$$

where c_∞ is the far-field solute concentration, a is an adjustable parameter which controls the magnitude of the anti-trapping current, the value of which will be discussed later, and u is a dimensionless variable given by

$$u = \ln\left(\frac{c}{c_\infty}\right) - \frac{1}{2} \ln k_E [h(\phi) + 1] \quad (8)$$

Here $h(\phi)$ is an interpolating function that satisfies $h(\pm 1) = \pm 1$.

The purpose of the anti-trapping current is to provide a solute flux normal to the diffuse interface from the solid into the liquid thus counterbalancing the tendency of phase-field models to display unphysically high levels of solute trapping. This tendency for *excess* solute trapping is an inherent property of diffuse interface models that do not include an anti-trapping current and gives rise to a level of solute trapping that is dependant upon the width chosen for the diffuse interface. As the interface width is generally set considerably larger than could be considered physical ($W \gg W_p$), excess amounts of solute trapping result.

Evaluating the variational derivative (4) and applying the non-dimensionalisations

$$U = \frac{e^u - 1}{1 - k_E}, \quad \theta = \frac{\Delta T - mc_\infty}{L/c_p} \quad \text{and} \quad M = -\frac{m(1 - k_E)}{L/c_p}, \quad (9)$$

where L is the latent heat on fusion and c_p is the specific heat, the phase and concentration equations may be obtained as^[10]

$$\tau \frac{\partial \phi}{\partial t} = W^2 \nabla^2 \phi - f'(\phi) - \lambda g'(\phi)(\theta + Mc_\infty U) \quad (10)$$

and

$$\frac{1+k_E}{2} \frac{\partial U}{\partial t} = \nabla \cdot \left(Dq(\phi) \nabla U + aW[1+(1-k_E)U] \frac{\partial \phi}{\partial t} \frac{\nabla \phi}{|\nabla \phi|} \right) + \frac{1}{2} \frac{\partial}{\partial t} \{h(\phi)[1+(1-k_E)U]\} \quad (11)$$

Here, λ is a coupling parameter and τ is a characteristic time for attachment at the interface, the values of which are given below. $g(\phi)$ is an interpolating function that satisfies the conditions $g(\pm 1) = \pm 8/15$ and $g'(\pm 1) = 0$.

Finally, the temperature equation is just the standard thermal diffusion equation with a source term, namely

$$\frac{\partial \theta}{\partial t} = \alpha \nabla^2 \theta + \frac{1}{2} \frac{\partial \phi}{\partial t} \quad (12)$$

In order to formulate the phase-field model in such a way that the results do not depend upon the width, W , of the diffuse interface the thin-interface analysis is applied, in which an asymptotic expansions of the solution (in p , a Péclet number based on the local interface velocity) on the inner and outer regions of the solid-liquid interface are matched to obtain an equation set in which the solution is independent of the width of the diffuse interface.

Physically, this analysis corrects for the effects of lateral concentration gradients along the interface, interface stretching (the fact that when curved a diffuse interface is longer on one side than the other) and the excess solute trapping described above. The analysis has previously been presented for a coupled model by [10], wherein results identical to that for the solute only case studied in [9] were recovered. For this reason we do not here repeat the analysis, only drawing attention to some points that we consider salient to a discussion of solute-trapping phenomena within the coupled phase-field model. Specifically, we note that the first order (in p) solutions for U and θ are,

$$U_1 = \bar{U}_1 + \frac{1}{2} [1 + (1 - k_E) U_0] \int_0^\eta \rho(\phi_0(\eta')) d\eta' \quad (13)$$

$$\theta_1 = \bar{\theta}_1 + A_\theta \eta + \frac{1}{2Le} \int_0^\eta \phi_0(\eta') d\eta' \quad (14)$$

where $\rho(\phi_0)$ is the function

$$\rho(\phi_0) = \frac{h(\phi_0) - 2a \frac{\partial \phi_0}{\partial \eta} - 1}{q(\phi_0)} \quad (15)$$

and ϕ_0 is the zero order solution in ϕ

$$\phi_0 = -\tanh\left(\frac{\eta}{\sqrt{2}}\right) \quad (16)$$

where η measures signed distance normal to the level line $\phi = 0$.

We note here that Eq. (13) is the same as that obtained for the thin interface analysis of the isothermal solute problem^[9]. If we now adopt $h(\phi) = \phi$ and $q(\phi) = 1/2(1-\phi)$ these being the simplest functions that satisfies the restrictions $h(\pm 1) = \pm 1$, $q(1) = 0$ and $q(-1) = 1$, and we take $a = 1/(2\sqrt{2})$ which has been shown *in the isothermal case* to eliminate the jump in chemical potentials on either side of the interface^[21, 9], we have $\rho(\phi_0) = (\phi_0 - 1)$. That is, the form of the integral in Eq. (13) reduces to the same form as that in Eq. (14), which is the also the same form as in the thin interface analysis of the pure thermal problem.

In the isothermal model other values of a are permitted should non-zero amounts of solute trapping be desired, a point specifically commented upon by [9], although this does require a re-evaluation of the integral

$$K = \int_{-\infty}^{+\infty} g'(\phi_0) \frac{\partial \phi_0}{\partial \eta} \left[\int_0^\eta \rho(\phi_0(\eta')) d\eta' \right] d\eta \quad (17)$$

However, in the coupled model the situation is more restrictive in that we require U_i and θ_i to have the same form in order for the analysis to be tractable, a point that is perhaps not clear in the derivation of the coupled model presented in [10], as the substitution $h(\phi) = \phi$ and $a = 1/(2\sqrt{2})$ have already been made when the integrals for U_1 and θ_1 are formulated. However, the implication of this is that once the choice $h(\phi) = \phi$ has been made, the thin interface analysis for the coupled thermo-solutal model can only be performed for $a = 1/(2\sqrt{2})$ and that this is therefore the only value for which the model is valid. Understanding how the anti-trapping current with $a = 1/(2\sqrt{2})$ effects the solute trapping behaviour of the coupled model is therefore an important issue.

3. Numerical Methods

Following the thin-interface analysis given in [10] we arrive at the equations governing the evolution of the coupled concentration, thermal and anisotropic phase fields, non-dimensionalised against the characteristic length and time scales W_0 and τ_0 respectively as,

$$A^2(\psi) \left[\frac{1}{Le} + Mc_\infty [1 + (1 - k_E)U] \right] \frac{\partial \phi}{\partial t} = \nabla \cdot (A^2(\psi) \nabla \phi) + \phi(1 - \phi^2) - \lambda(1 - \phi^2)^2 (\theta + Mc_\infty U) - \frac{\partial}{\partial x} \left(A(\psi) A'(\psi) \frac{\partial \phi}{\partial y} \right) + \frac{\partial}{\partial y} \left(A(\psi) A'(\psi) \frac{\partial \phi}{\partial x} \right) \quad (18)$$

$$\left(\frac{1 + k_E}{2} - \frac{1 - k_E}{2} \phi \right) \frac{\partial U}{\partial t} = \nabla \cdot \left(\tilde{D} \frac{1 - \phi}{2} \nabla U + a |1 + (1 - k_E)U| \frac{\partial \phi}{\partial t} \frac{\nabla \phi}{|\nabla \phi|} \right) + \frac{1}{2} \left(|1 + (1 - k_E)U| \frac{\partial \phi}{\partial t} \right) \quad (19)$$

$$\frac{\partial \theta}{\partial t} = \tilde{\alpha} \nabla^2 \theta + \frac{1}{2} \frac{\partial \phi}{\partial t} \quad (20)$$

where $\psi = \arctan(\phi_x/\phi_y)$ is the angle between the normal to the interface and the x -axis, $A(\psi) = 1 + \varepsilon \cos(\eta\psi)$ is an anisotropy function with strength ε and mode number η and $\tilde{D} = D\tau_0/W_0^2$ and $\tilde{\alpha} = Le.D$ are the dimensionless solute and thermal diffusivities respectively. The characteristic length and time scales are given by

$$W_0 = \frac{d_0 \lambda}{a_1}, \quad \tau_0 = \frac{d_0^2 a_2 \lambda^3}{Da_1^2}. \quad (21)$$

The dimensionless coupling parameter, λ , results from the thin interface analysis and is given as^[9, 10],

$$\lambda = \frac{\tilde{D}}{a_2} = \frac{a_1 W_0}{d_0} \quad (22)$$

where d_0 is the chemical capillary length and the constants a_1 and a_2 are given by [9] as $a_1 = \frac{5\sqrt{2}}{8}$ and

$$a_2 = 0.6267.$$

The governing equations are discretized using a finite difference approximation based upon a quadrilateral, non-uniform, locally-refined mesh with equal grid spacing in both directions. This allows the application of standard second order central difference stencils for the calculation of first and second differentials, while a compact 9-point scheme has been used for Laplacian terms, in order to reduce the mesh induced^[22] anisotropy. The mesh data is stored in a quadtree data structure as in [23, 24].

In order to ensure that sufficient levels of refinement occur around the interface region and that the extreme multi-scale nature of the thermal and solutal diffusion fields are handled appropriately, local mesh refinement (coarsening) is employed when the weighted sum of the gradients of ϕ , U or θ exceeds (falls below) some predefined value.

As discussed elsewhere^[25, 26] if explicit temporal discretization schemes are used for this problem the maximum stable time-step is given by $\Delta t \leq Ch^2$, where $C = C(\lambda, Le, \Delta T)$, with $C \leq 0.001$ found under certain conditions leading to unfeasibly small time-steps. Consequently, an implicit temporal discretization is employed here based on the second order Backward Difference Formula, which is an implicit linear 2-step method, with variable time-step.

When using implicit time discretisation methods on heavily refined finite difference grids it is necessary to solve a very large, but sparse, system of non-linear algebraic equations at each time-step. Multigrid methods are among the fastest available solvers for such systems and in this work we apply the non-linear generalization known as FAS (full approximation scheme [27]). The local adaptivity is accommodated via the multilevel algorithm originally proposed by Brandt^[28]. The interpolation operator is bilinear while injection is used for the restriction operator. For smoothing the error we use a fully-coupled nonlinear weighted Gauss-Seidel iteration where the number of pre- and post-smoothing operations required for optimal convergence has been investigated within the context of phase-field simulation in [11, 12]. Based on that work we have used V-cycle iterations with 2 pre- and 2 post- smoothing operations at each level. A major property of the multigrid method is h -independent convergence, which means that the convergence rate does not depend on the element size. This behaviour is vital in respect of being able to solve the extreme multi-scale problem arising from coupled thermo-solutal phase-field simulations. Full details of the numerical scheme are given in [11, 12]

4. Results

Validation of our numerical scheme against both other coupled phase-field models^[7, 10] and, where available, against analytical solutions for pure thermal and pure solutal growth have been reported previously^[11, 12, 26], and is therefore not repeated here. The correct implementation of the anti-trapping current within the model has been validated by reducing the coupled model to the pure solutal case at solutal undercooling Ω by setting $1/Le \rightarrow 0$, removing Eq. (20) from the equation set and fixing the system temperature everywhere at $\theta_{\text{sys}} = -\Omega$ with $Mc_\infty = 1 - (1-k_E)\Omega$ [see 25]. By so doing it is possible to explore the behaviour of the anti-trapping current during the growth of a dendrite under solute only control, wherein we find, in agreement with [9], that solute trapping is suppressed and that the curvature corrected partition coefficient

$$\frac{c_s}{c_l^0} = k[1 - (1-k)\frac{d_0}{\rho}] \quad (23)$$

recovers the equilibrium partition coefficient, k_E , to a very high degree of precision. Specifically, for $\Omega = 0.15$ and $k_E = 0.3$ we recover $k = 0.3000 \pm 0.0001$ at a growth velocity Vd_0/D of order 2×10^{-4} , where this has been tested for λ between 1 and 5 and for h between 0.78 and 0.19 (corresponding to 11 to 13 levels of refinement respectively on a domain of $[-800,800]^2$).

We now consider the partitioning behaviour of the model when we allow a dendrite to grow under coupled thermo-solutal control. Fig. 1 shows the measured (curvature corrected) partition coefficient for a large number of simulations as a function of the dimensionless velocity. All the simulations in this sequence have $k_E = 0.3$, $Mc_\infty = 0.05$, $\lambda = 5$ and $\gamma = 0.02$ and were run with a fixed minimum grid spacing of $h = 0.78$, although the domain size varied between simulations such that interactions between the domain boundary and the thermal field were not encountered. The growth velocity of the dendrite was controlled by varying the undercooling, Δ , in the range 0.1 – 0.8. Lewis numbers in the range 200 - 10000 were considered and are denoted by the symbols in the figure. For comparison, one set of simulations performed in the absence of an anti-trapping current is also shown. In all cases we have estimated the error in determining k as being $\sim \pm 2.5\%$. This is based primarily on the uncertainty in determining the value of c_l^0 at the interface, this being a steeply peaked function. This indicative error has been shown on a number of representative points.

A number of points are apparent from the figure. Firstly, it is clear that despite the presence of an anti-trapping current the measured partition coefficient varies strongly as a function of velocity, with the equilibrium value, k_E , only being recovered as the velocity tends to zero. We do however note that the growth velocity in the coupled model does tend to be much higher than in the pure solutal model, particularly at high Lewis number. Secondly, although we have shown elsewhere^[26] that the actual growth velocity is a strong function of Le , no explicit Lewis number dependence is observed, with all the points corresponding to Lewis numbers in the range 200-10 000 laying, to a very good approximation, on the same curve.

As described above, in experimental solidification studies the observed velocity dependant partition coefficient, $k(V)$, is described by the relationship due to Aziz^[13, 14] given in Eq. (2). Should this relationship also hold for the phase-field model, plotting the group $\{(k-k_E)/(1-k)\}$ against V should yield a straight line with gradient $1/V_D = W_0/D_i$. A plot of this type is shown in Fig. 2, where we now also include data for values of the coupling parameters, λ , of 1 and 2 as well as the data shown previously for $\lambda = 5$ (which, through Equ. (22) is equivalent to setting the diffuse interface width, W_0 , to 1.13, 2.62 and 5.65 times d_0 respectively). As before all simulations are run with $k_E = 0.3$, $Mc_\infty = 0.05$, $\gamma = 0.02$ and with a minimum h of 0.78. The Lewis number in the simulations is, as before, in the range 200 - 10 000, although for clarity we have not indicated the Lewis number in the plot. This is reasonable as we have already demonstrated above that there is no explicit Lewis number dependency. A number of points are apparent from the figure.

Firstly, despite being formulated within the thin interface limit described by [9, 10] the model does have an interface width dependence in so much as solute-trapping is concerned, with a more diffuse interface giving rise to higher levels of solute-trapping. Despite this, in respect of the other main predictive quantities obtained from the model (i.e. V , ρ) the results obtained from the model are indeed independent of the width of the diffuse interface. This has been shown both by Ramirez & Beckermann^[7] and ourselves^[12, 25], with further evidence being presented in Figure 3, where we show that models with different values of λ , and which therefore display different solute trapping characteristics, give mutually consistent values for V and ρ . Note that here, due to the requirement to keep the group $W_0V/D < 1$ ^[21], the range of accessible values of V decreases as λ increases.

The second point that we note is that the data do, to a reasonable approximation, fit the Aziz model in respect of their velocity dependence. Moreover, if we fit linear regression models to the data sets we obtain gradients in each of the three cases of 0.56, 1.09 and 2.75 (for $\lambda = 1, 2$ and 5 respectively), these values displaying an almost exact 1 to 2 to 5 ratio. Equating these gradients with W_0/D_i and applying the standard non-dimensionalisation described in Section 2 we obtain $\tilde{D}_i = 1.81$. Similar results can be obtained by varying λ over a wider parameter space while keeping all other parameters, including Δ , fixed, an example of which is shown in Fig. 4. Here the model parameters are $k_E = 0.3$, $Mc_\infty = 0.05$, $\gamma = 0.02$, $\Delta = 0.25$, $Le = 200$ and we have plotted the group $\{(k - k_E)/\tilde{V}(1 - k)\}$ against λ so that, as above, the gradient may again be directly associated with $1/\tilde{D}_i$, to obtain $\tilde{D}_i = 1.91$.

However, it is apparent from Fig. 4 (and also to a lesser degree Fig. 2) that the coupled phase-field model here does not quite reproduce the expected Aziz solute trapping law. Specifically, we would expect that the group $(k - k_E)/V(1 - k)$ should show a linear dependence on W_0 (and hence λ , see solid line in Fig. 4). Although this is approximately true, it appears from Fig. 4 that a small quadratic correction may also be present (dashed line). Recently, Ohno & Matsuura^[29] have shown that an additional term may be applied to the anti-trapping current. Although their work is predominantly aimed at developing a formulation of j_{at} for models with a non-zero solute diffusivity in the solid, their formalism suggests that the term a be modified, so that under the conditions applied here with zero solute diffusivity in the solid it would read

$$a = \frac{1}{2\sqrt{2}} \left(1 - \frac{\chi(s)}{2} \right) \quad (24)$$

where χ is related to the concentration gradient on the solid side of the interface and the local velocity of the interface, both of which will be functions of s , the arc length along the interface. We speculate that this more complex form for a may potentially correct this small quadratic anomaly in the observed solute trapping behaviour. There are however problems with the extended form of the anti-trapping current. Even for the isothermal model the explicit dependence of χ upon s is not specified, and for a non-planar interface would require prior knowledge of the solution. Moreover, in the coupled thermo-solutal case the requirement that

Equations (13) and (14) (for U_1 and θ_1 respectively) have the same form would probably render the thin-interface analysis intractable for this more complex form for a .

Given that we have shown above that the coupled thermo-solutal model (i) still displays solute trapping and (ii) that the level of solute trapping (but neither V nor ρ) display an interface width dependence it is perhaps pertinent to explore what effect the anti-trapping current, j_{at} , is having upon the model. This has been done by varying the parameter a in Eq. (7). The results are shown in Fig. 5, in which we show k as a function of a , corresponding to three sets of simulations with $\Delta = 0.25$ all other parameters being as reported above with the exception of Mc_∞ , which controls the relative importance of the thermal and solutal effects. The values used are $Mc_\infty = 0.02, 0.05$ and 0.1 . We observe that the partition coefficient varies, to a very good approximation, linearly with a in all three cases, and solute trapping appears to be totally suppressed (the equilibrium value of k , k_E , is recovered) for $a \sim 1/\sqrt{2}$. This is approximately twice the value required in Eq. (15) in order that in the thin interface analysis and the matched asymptotic expansions for the thermal and solutal fields have the same form. There is some indication of a small systematic variation, with slightly lower values of a recovering equilibrium partitioning behaviour (no solute trapping) in more concentrated alloys, although the size of the effect is such that we cannot completely rule out there being no concentration effect, nor that the value of a required to eliminate solute trapping is exactly $1/\sqrt{2}$. Interestingly, when an analysis similar to that presented in Fig. 4 is conducted without an anti-trapping current being present, an exact linear proportionality relationship is recovered, with $\tilde{D}_i = 0.55$.

However, we would stress that the thin interface analysis that renders V and ρ independent of the interface width is only valid for $a = 1/(2\sqrt{2})$. This is illustrated in Fig. 6 where we show, for the simulation with $Mc_\infty = 0.05$ that the Péclet number varies by a factor 1.5 in the range $0 \leq a \leq 1/\sqrt{2}$, while σ^* varies by a factor of 3. Similar levels of variation are observed at $Mc_\infty = 0.02$ and 0.1 . This is a much more significant variation than in the solute only model where the Péclet number is almost independent of a while σ^* varies by less than 25% over the range $0 \leq a \leq 1/\sqrt{2}$. Moreover, for the solute only model, setting $a = 1/\sqrt{2}$ (i.e. twice its standard value) results in the unphysical situation (for $k_E < 1$) that the measured value of k is lower than its equilibrium value, with the extent of this unphysical behaviour increasing with increasing Ω (over the range tested of 0.15-

0.8). That is, the higher the growth velocity the more the curvature corrected partition coefficient drops below its equilibrium value. Consequently, the behaviour of the coupled model appears fundamentally different to that of the solutal model.

5. Summary and Conclusions

We have used the phase field model due to Ramirez & Beckermann^[7, 10], modified to include an implicit solution capability, to explore how the inclusion of an anti-trapping current within a model of coupled thermo-solutal growth formulated in the thin interface limit actually affects the levels of solute trapping observed during dendritic growth. Contrary to published results for pure solutal models we find that the inclusion of such an anti-trapping current does not lead to the recovery of the equilibrium partition coefficient, except for the limiting case of vanishing growth velocity. At non-zero growth velocities non-vanishing amounts of solute trapping are observed. Moreover, the extent of this solute trapping is dependant upon the width of the mesoscopic diffuse interface. Indeed, to a good approximation we find that our model recovers the Aziz solute trapping law with a constant interface diffusivity, that is that the solute trapping behaviour may be expressed as a function of the group $\beta = VW_0/D_i$. This result has significant implications for our understanding of the coupled thermo-solutal model.

Specifically, the coupled thermo-solutal model, when formulated in the thin-interface limit, appears to behave very differently to its pure solutal counterpart, in that for solute only transport the inclusion of an anti-trapping current with $a = 1/(2\sqrt{2})$ will completely suppress solute trapping such that the equilibrium partition coefficient is recovered when curvature effects are properly accounted for. In the coupled model this appears not to be the case, with the anti-trapping current (with $a = 1/(2\sqrt{2})$) reducing the extent of solute trapping to approximately half of its value if such a current were not included. That is not to say however that for quantitatively valid solutions in the thin-interface limit the anti-trapping current can be neglected, nor indeed can its value be altered, as the matched asymptotic expansion of the inner and outer regions of the solution are only tractable for this ‘magic’ value of $a = 1/(2\sqrt{2})$. Consequently, although total suppression of solute trapping can be achieved for $a = 1/\sqrt{2}$, this has little practical value as both V and ρ (and consequently σ^*) show a strong

dependence upon a , with the asymptotic analysis suggesting that values of V and ρ obtained away from $a = 1/(2\sqrt{2})$ are erroneous.

However, we view the fact that the coupled model retains finite levels of solute trapping, particularly at high growth velocity, as being a strength, rather than a weakness. For solute only growth in the isothermal limit (which implicitly assumes that solidification velocities are very low) the prediction of solute trapping is erroneous as experimentally it would not be expected. In contrast, in the coupled model the failure to predict solute trapping at high undercoolings would be erroneous as this would not accord with observation during rapid solidification processing^[30, 31] where growth velocities can exceed 150 m s^{-1} [32]. In such situations very high levels of solute trapping are observed.

Moreover, it has hitherto been assumed that provided the phase-field model is constructed within the thin interface formalism, quantitatively valid results may be obtained independent of the width of the diffuse interface, leaving this parameter to be chosen for computational expediency. We now show that this strictly is not the case and that actually λ , and hence W_0 , should be chosen so as to match the expected levels of solute trapping. In fact, this is not a particularly stringent condition as both the results presented here and elsewhere [7, 10, 12] suggest that V , ρ and σ^* do not show a strong dependence on λ , and therefore that they are only weakly effected by solute trapping. This will be particularly true at low undercoolings, where the levels of solute trapping are expected to be low. Conversely, at higher undercoolings and where quantitative predictions of segregation behaviour are required λ may no longer be considered to be a free parameter, wherein it becomes appropriate to enquire as to the appropriate value of λ to yield quantitatively valid solute trapping results.

However, obtaining quantitative evidence for what might constitute an appropriate level of solute trapping is far from straight forward. Experimentally, this is generally presented as a diffusive velocity ($V_D = D_i/W_p$), with estimates varying by up to two orders of magnitude in closely related systems (e.g. from $V_D = 0.37 \text{ m s}^{-1}$ in Si-As [33] to $V_D = 32 \text{ m s}^{-1}$ in Si-Bi [34]). Moreover, there is the possibility that V_D is dependant upon k_E , with values of k_E close to unity giving values of V_D towards the lower end of the spectrum of values. For metal (Al) based systems, which is probably the closest match to the parameter set used here, [35] have reported values for V_D that may be around $5\text{-}20 \text{ m s}^{-1}$. Using the results from above we would estimate the equivalent (dimensional) diffusive velocity operating here as $(1.91/W_0)D/d_0$. We have shown previously^[26] that the parameter set used

here is consistent with Cu- 5wt.% Ni, wherein we obtain $D \approx 3.2 \times 10^{-9} \text{ m}^2\text{s}^{-1}$ [36] and $d_0 = 3.7 \times 10^{-10} \text{ m}$ [37] or $V_D \approx (19/W_0) \text{ m s}^{-1}$. This would suggest that W_0 should be adjusted to be between 1-3 d_0 to give realistic values of solute trapping.

6. References

1. A.A. Wheeler, B.T. Murray & R.J. Schaefer, *Physica D* 66 (1993) 243.
2. A.M. Mullis & R.F. Cochrane, *Acta Mater.* 49 (2001) 2205.
3. J.A. Warren & W.J. Boettinger, *Acta Metall. Mater.* 43 (1995) 689.
4. J.R. Green, A.M. Mullis & P.K. Jimack, *Metall. Mater. Trans. A* 38 (2007) 1426.
5. I. Loginova, G. Amberg & J. Aagren, *Acta Mater.* 49 (2001) 573.
6. J.A. Warren & W.J. Boettinger, *Acta Metall. Mater.* 43 (1995) 689.
7. J.C. Ramirez & C. Beckermann, *Acta mater.* 53 (2005) 1721.
8. C.W. Lan, Y.C. Chang, C.J. Shih, *Acta mater.* 51 (2003) 1857.
9. A. Karma, *Phys. Rev. Lett.* 87 (2001) 115701.
10. J.C. Ramirez, C. Beckermann, A. Karma & H.-J. Diepers, *Phys. Rev. E* 69 (2004) 051607.
11. J. Rosam, P.K. Jimack & A.M. Mullis, *J. Comp. Phys.* 225 (2007) 1271.
12. J. Rosam, P. K. Jimack & A. M. Mullis, *Acta Mater.* 56 (2008) 4559.
13. M.J. Aziz, *J. Appl. Phys.* 53 (1982) 1158.
14. M.J. Aziz, *Mater. Sci. Eng. A* 178 (1994) 167.
15. A.A. Wheeler, W.J. Boettinger & G.B. McFadden, *Phys. Rev. E* 47 (1993) 1893.
16. N.A. Ahmad, A.A. Wheeler, W.J. Boettinger & G.B. McFadden. *Phys. Rev. E* 58 (1998) 3436.
17. D. Danilov & B. Nestler, *Acta Mater.* 54 (2006) 4659.
18. S.G. Kim, W.T. Kim & T. Suzuki, *Phys. Rev. E* 60 (1999) 7186.
19. K. Galsner, *Physica D* 151 (2001) 253.
20. M. Conti, *Phys. Rev. E* 56 (1997) 3717.
21. B. Echebarria, R. Folch, A. Karma & M. Plapp, *Phys. Rev. E* 70 (2004) 061604.
22. A.M. Mullis, *Comp. Mater. Sci.* 36 (2006) 345.
23. N. Provatas, N. Goldenfeld & J. Dantzig, *J. Comp. Phys.* 148 (1999) 265.

24. A. Jones & P.K. Jimack, *Int. J. Num. Meth. Fluids* 47 (2005) 1123.
25. J. Rosam, PhD Thesis, University of Leeds, Leeds LS2-9JT.
26. J. Rosam, P. K. Jimack & A. M. Mullis, *Phys. Rev. E* 79 (2009) 030601.
27. U. Trottenberg, C. Oosterlee & A. Schuller, *Multigrid*, Academic Press (2001).
28. A. Brandt, *Math. Comp.* 31 (1977) 333.
29. M. Ohno & K. Matsuura, *Phys. Rev. E* 79 (2009) 031603.
30. K.I. Dragnevski, A.M. Mullis, Walker D.J. & R.F. Cochrane, *Acta Mater.* 50 (2002) 3743.
31. S.E. Battersby, R.F. Cochrane & A.M. Mullis, *Mater. Sci. Eng. A* 226 (1997) 443.
32. K.I. Dragnevski, R.F. Cochrane & A.M. Mullis, *Phys. Rev. Lett.* 89 (2002) 215502.
33. J.A. Kittl, P.G. Sanders, M.J. Aziz, D.P. Brunco & M.O Thompson, *Acta Mater.* 48 (2000) 4797.
34. M.J. Aziz, J.Y. Tsao, M.O. Thompson, P.S. Peercy & C.W. White, *Phys. Rev. Lett.* 56 (1986) 2489.
35. P.M. Smith, R. Reitano & M.J. Aziz, *Mater. Res. Soc. Symp. Proc.* 279 (1993) 749.
36. X.J. Han, M. Chen & Y.J. Lu, *Int. J. Thermophys.* 29 (2008) 1408.
37. *Smithells Metals Reference Book 7th Edition* (Eds. E.A. Brandes & G.B. Brook), Butterworth-Heinemann (1992).

Figure Captions

Fig. 1. Measured partition coefficient, k , as a function of growth velocity for the coupled thermo-solutal phase-field model with $k_E = 0.3$, $Mc_\infty = 0.05$, $\lambda = 5$ and $\gamma = 0.02$, with Lewis number in the range 200-10000. Velocity is varied via altering the undercooling Δ . The estimated uncertainty of $\pm 2.5\%$ applied to all points, but for clarity is shown only for selected points.

Fig. 2. Solute partitioning behaviour as a function of velocity showing good general agreement with the Aziz model and a dependence upon coupling parameter, λ , (and hence diffuse interface width). As above, uncertainty is estimated at $\pm 2.5\%$.

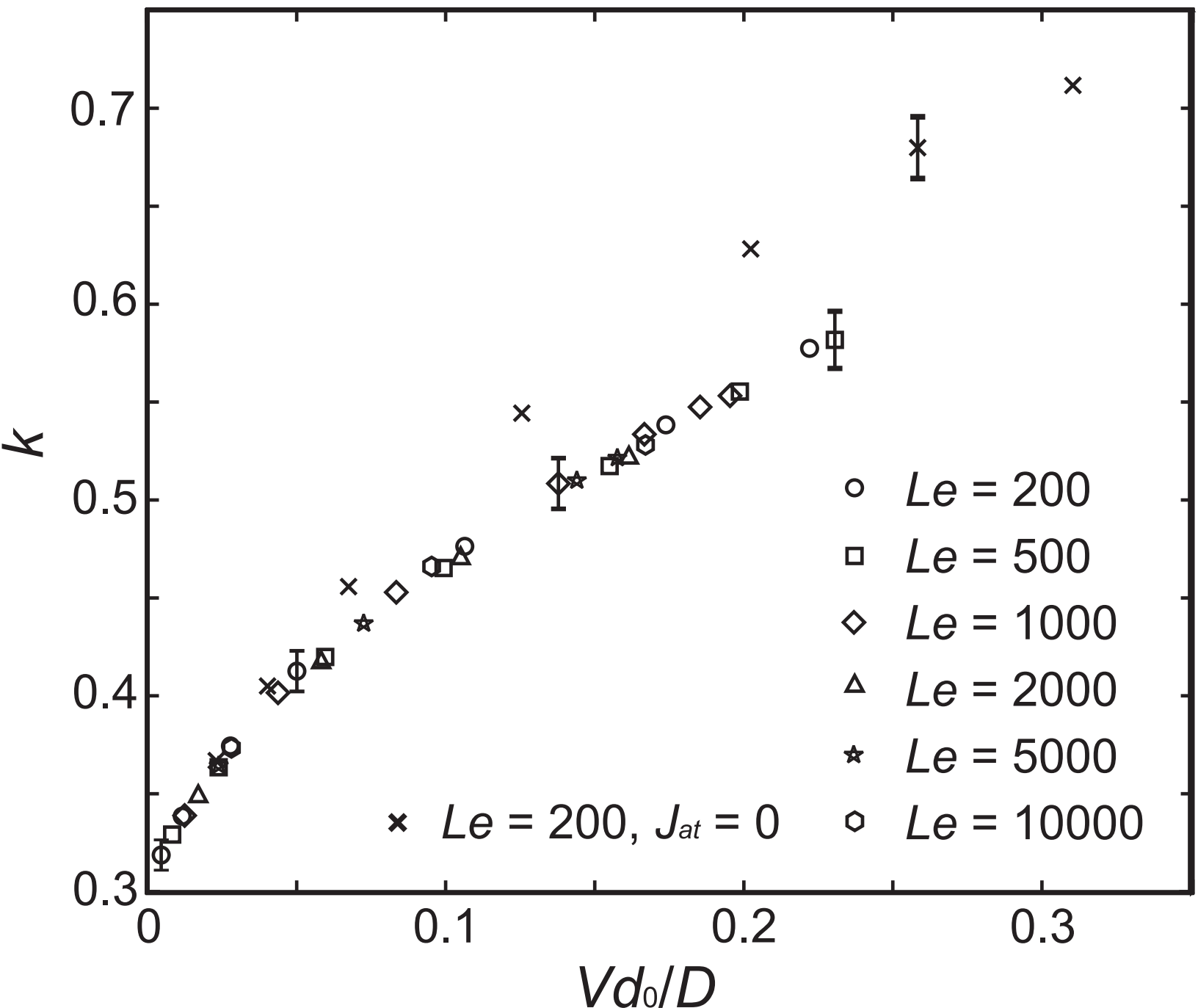
Fig. 3. Dendrite tip radius as a function of velocity for different values of λ , showing that although λ effects the solute trapping characteristics of the dendrite, mutually consistent values for the tip velocity and radius are obtained independent of the value used for λ .

Fig. 4. Solute partitioning behaviour as a function of the coupling parameter, λ , showing good general agreement with the Aziz model.

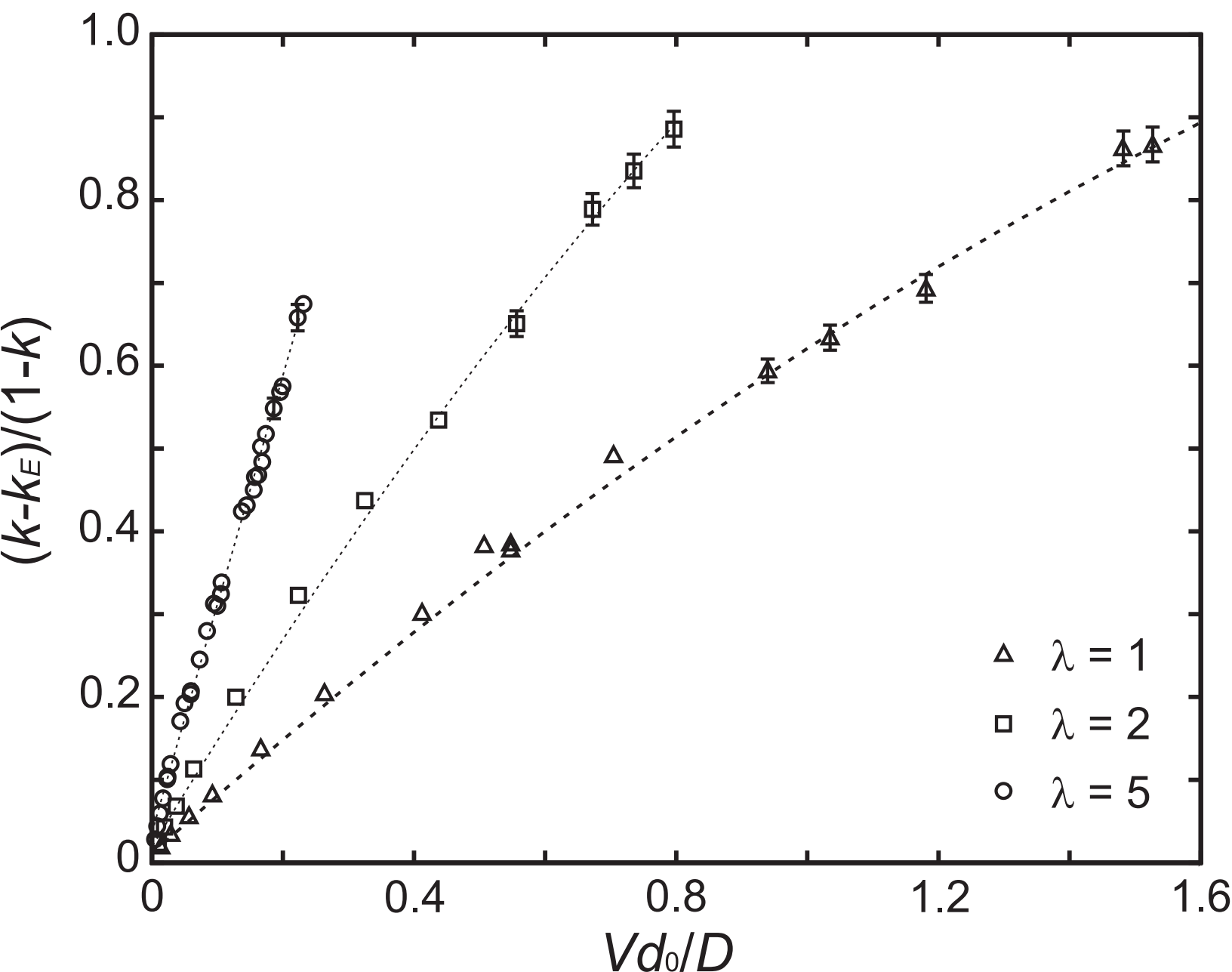
Fig. 5. Value of the measured partition coefficient, k , as a function of the anti-trapping parameter a , for a coupled model with $\Delta = 0.25$ and $k_E = 0.3$. Three values of the concentration parameter, Mc_∞ , are considered, 0.02, 0.05 and 0.1. Note that the equilibrium value, k_E , is, in each case recovered for approximately double the value of $a = 1/2\sqrt{2}$ for which the thin-interface analysis is valid.

Fig. 6. Values of the Péclet number (left-hand axis) and radius selection parameter (right-hand axis) as a function of anti-trapping parameter a , illustrating that this cannot be treated as a free parameter to control solute trapping while retaining quantitatively valid solutions for V and ρ . Model parameters are $Mc_\infty = 0.05$, $\Delta = 0.25$ and $k_E = 0.3$.

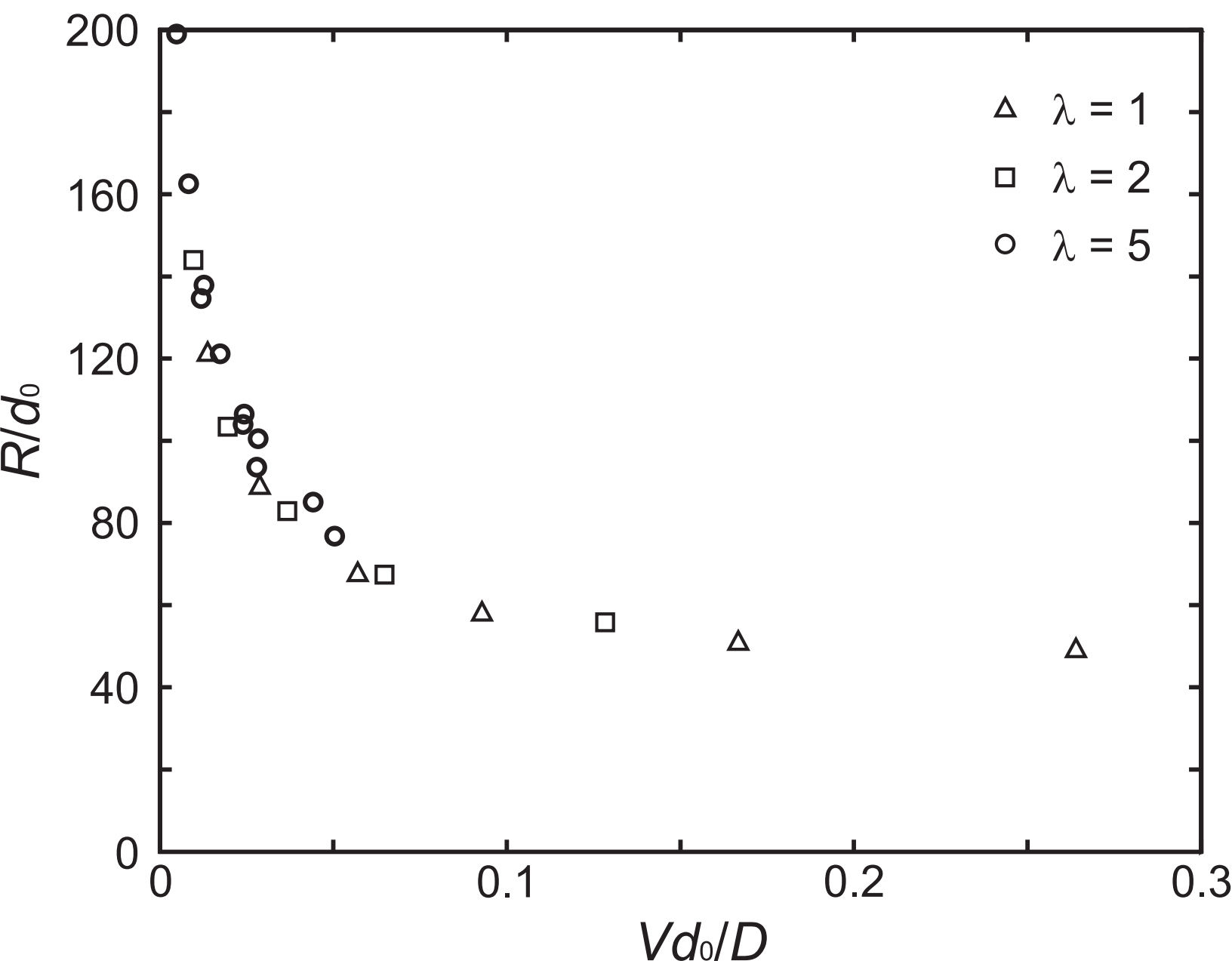
6. Figure #1



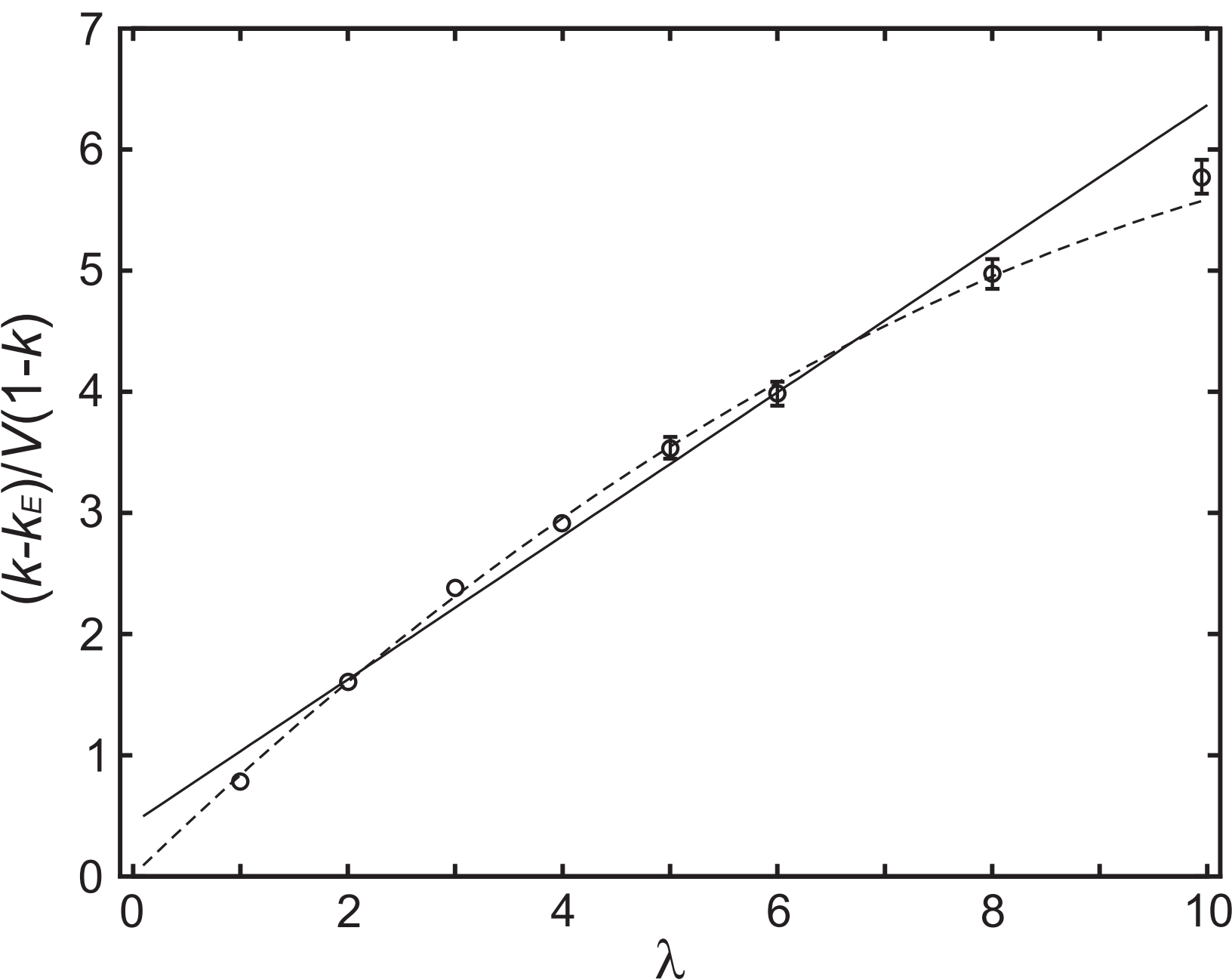
6. Figure #2



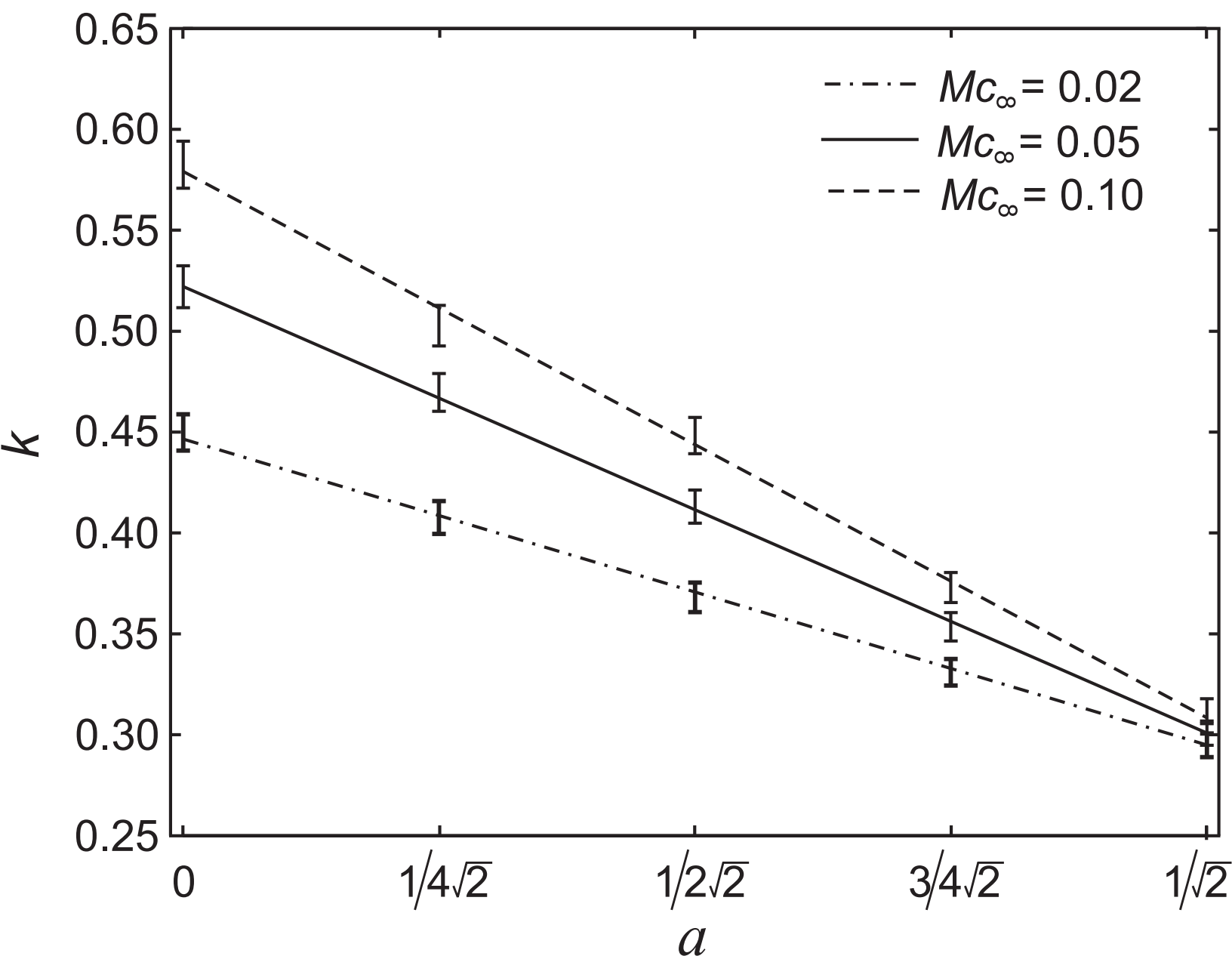
6. Figure #3



6. Figure #4



6. Figure #5



6. Figure #6

